

## Large intrinsic effect of axial strain on the critical current of high-temperature superconductors for electric power applications

D. C. van der Laan<sup>a)</sup> and J. W. Ekin

National Institute of Standards and Technology, Boulder, Colorado 80305

(Received 3 November 2006; accepted 20 December 2006; published online 31 January 2007)

A remarkably large reversible reduction in the critical current of “second generation” high-temperature superconductors for electric power applications has been measured with a new technique over a wide range of mechanical strain. The effect amounts to a 40% reduction in critical current at 1% compressive strain in self-magnetic field, and is symmetric for compressive and tensile strains. The intrinsic effect is measured in highly aligned multigranular  $\text{YBa}_2\text{Cu}_3\text{O}_{7-d}$  coated conductors made by different processes, including superconductors with nanoscale pinning centers. This effect and its magnitude are expected to have a significant impact on power applications and provide a useful new parameter for probing the fundamental nature of current transport in high-temperature superconductors. [DOI: 10.1063/1.2435612]

Considerable technical advances have been achieved during the past several years in the development of high-temperature superconductors (HTSs) for use in large-scale applications.<sup>1</sup> Research efforts have resulted in superconducting current densities ( $J_c$ ) in  $\text{YBa}_2\text{Cu}_3\text{O}_{7-\delta}$  (YBCO) coated conductors of 2.5–3.0 MA/cm<sup>2</sup> in self-magnetic field at 77 K, in conductor lengths exceeding 300 m.<sup>2</sup> Also, major advances in the ability of HTS to carry a supercurrent at high magnetic field have been achieved by enhancing their flux pinning properties by introducing nanoscale defects.<sup>3–5</sup> However, not only the electrical performance of the conductors is important for applications but also the conductor’s performance when subjected to the mechanical strains expected in service.

The effect of strain on the critical current has governed the design of low-temperature superconductor applications for decades. No reversible change in  $J_c$  with strain was observed in HTSs in the first 17 years after their discovery in 1986. The superconducting current density of these brittle, ceramic materials is affected very little by limited strains (0.2%–0.4%), and, at higher strains,  $J_c$  was observed to degrade irreversibly when the ceramic current paths start to fracture.<sup>6,7</sup> A possible reversible strain effect in the limited elastic strain regime of early materials was most likely masked by the multiplicity of current paths that result from the granularity of the materials and their rather poor grain alignment.

A relatively small reversible strain effect under tension was first discovered in HTS in YBCO coated conductors in 2003.<sup>8</sup> Its observance is ascribed largely to an improved grain-to-grain alignment in superconducting films [within about 6° full width at half maximum (FWHM)] when deposited on a metal substrate with ceramic buffer layers (“coated conductors”). The effect of the strain on the critical current was limited in magnitude, amounting to a  $J_c$  decrease of about 5%.<sup>9,10</sup>

The grain alignment in YBCO coated conductors improved even further during the last two years and is mainly responsible for the larger superconducting current densities of 2.5–3.0 MA/cm<sup>2</sup> at 77 K in self-field. These highly

aligned conductors (within 3°–5° FWHM) are currently being produced in lengths exceeding 300 m and have provided the ability to conduct a higher strain investigation of the reversible strain effect without encountering irreversible fracturing of the superconducting film.<sup>2</sup> Here we report on a reversible strain effect in highly aligned YBCO coated conductors that is surprisingly consistent and of a magnitude that has not been seen before in high-temperature superconductors.

Three types of coated conductors were investigated. The first consists of ceramic buffer layers deposited on a 50  $\mu\text{m}$  thick Hastelloy C-276 substrate and a 1  $\mu\text{m}$  thick YBCO layer deposited on top of the buffer layers by metal-organic chemical-vapor deposition (MOCVD).<sup>11,12</sup> Coated conductors of this type have a columnar YBCO grain structure. Grain alignment is introduced into the MgO buffer layer with ion-beam-assisted deposition (IBAD),<sup>13</sup> which results in an average in-plane grain alignment in the YBCO layer of 3°–4° FWHM. A 2  $\mu\text{m}$  thick silver cap layer is deposited on top of the YBCO layer for electrical and thermal stabilities. These samples are designated MOCVD-IBAD. Some of the MOCVD-IBAD samples are surround plated with 20  $\mu\text{m}$  of copper for additional stability.

The second type of coated conductor investigated consists of a 0.8  $\mu\text{m}$  thick YBCO layer deposited onto a buffer substrate with metal-organic deposition (MOD).<sup>14,15</sup> This technique results in a laminar YBCO grain structure with meandering grain boundaries.<sup>16</sup> Grain alignment is introduced with a 75  $\mu\text{m}$  thick textured NiW substrate, produced by a rolling-assisted-biaxially textured-substrate (RABiTS) technique,<sup>17,18</sup> which results in an average in-plane grain alignment of the top  $\text{CeO}_2$  buffer layer of 4.5°–5.5° FWHM. A 3  $\mu\text{m}$  thick silver cap layer is deposited on top of the YBCO layer for stability. These samples are designated as MOD-RABiTS.

The third type of conductor investigated is of the MOD-RABiTS type, but fabricated with a double YBCO layer. It consists of a 0.8  $\mu\text{m}$  thick layer of YBCO that is doped with a large amount of Dy nanoparticles that provide extra pinning centers.<sup>18</sup> A 0.6  $\mu\text{m}$  thick undoped YBCO layer is then deposited on top of the doped layer in a second step. These samples are designated as hybrid MOD-RABiTS. Additional

<sup>a)</sup>Electronic mail: danko@boulder.nist.gov

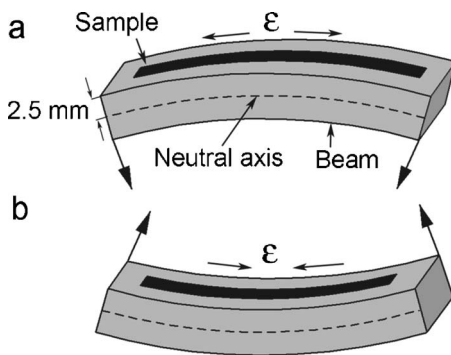


FIG. 1. Illustration of method for applying large axial strains to the superconducting sample, which is soldered on top of a Cu 2 wt % Be bending beam. Axial tension is applied by bending the beam in the direction shown in (a), whereas axial compression is applied by bending the beam in the opposite direction (b).

stability is provided to some of the MOD-RABiTS samples by soldering two 50  $\mu\text{m}$  thick copper strips on both sides of the sample.

The superconducting current density was measured as a function of both high compressive strain and high tensile strain with a Cu 2 wt % Be beam in a four-point bending apparatus at 76 K. Axial strain is applied to the sample, which is soldered onto the bending beam, as illustrated in Fig. 1. Critical current density is determined with a voltage criterion of 1  $\mu\text{V}/\text{cm}$  and an uncertainty of about  $\pm 1\%$ . The axial strain in the 0.8–1.4  $\mu\text{m}$  thick YBCO layer is measured with a strain gauge and is homogeneous over the thickness of the YBCO film to within one part in 1900–3300 (ratio defined by the thickness of the YBCO layer and the distance of the layer from the neutral axis of the beam).

Figure 2 shows the results for the MOD-RABiTS samples. Under axial compressive strain, a reversible reduction of over 40% is measured at a compressive strain of  $-0.95\%$ , which has never been measured in HTS before. The

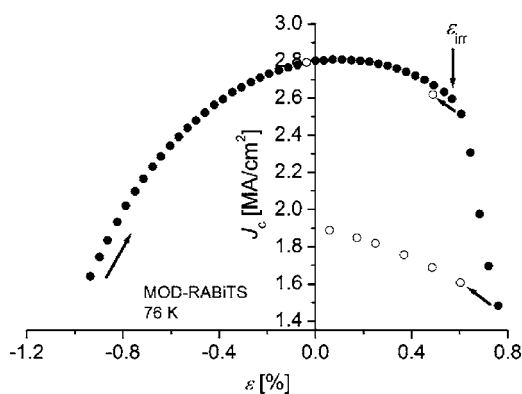


FIG. 2. Dependence of the superconducting current density on applied axial strain in a copper laminated MOD-RABiTS sample at 76 K. The measurement was first taken at axial compressive strains (left side of plot), and  $J_c$  is plotted as a function of strain, as shown by solid symbols. The applied compressive strain was released from  $-0.95\%$  (as indicated by the left arrow) and  $J_c$  was remeasured at zero applied strain (open symbol near  $\varepsilon=0$ ). The applied strain did not return to zero, because of yielding in the sample substrate. The bending beam was then turned over in the four-point bender, while still submerged under liquid nitrogen, and  $J_c$  was measured as a function of tensile strain (again shown by solid symbols on the right side of the plot). The superconducting current density starts degrading irreversibly at an applied tensile strain indicated by  $\varepsilon_{\text{irr}}$ . The irreversible loss of critical current becomes evident when strain is partly released and  $J_c$  is measured again (open symbols on the right side the plot).

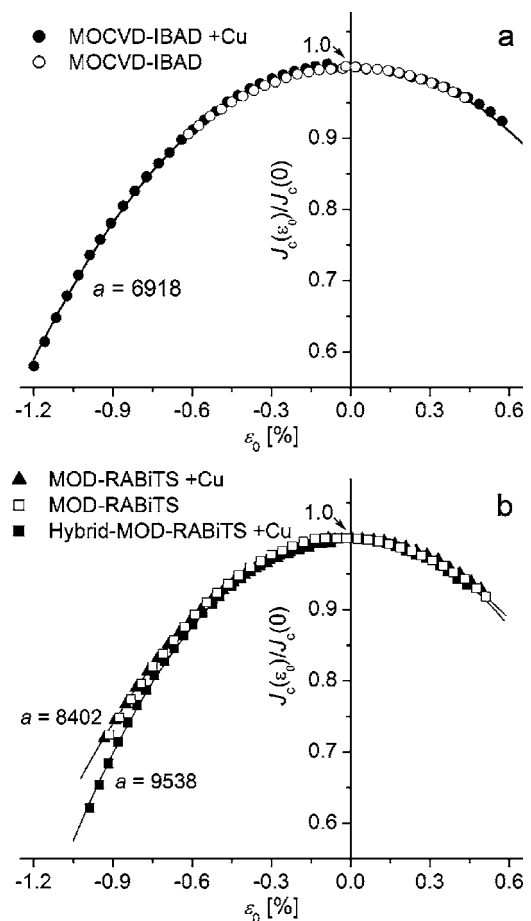


FIG. 3. Normalized superconducting current density is plotted as function of intrinsic strain  $\varepsilon_0$  over the range where  $J_c$  changes reversibly for MOCVD-IBAD samples in (a) and for (hybrid) MOD-RABiTS samples in (b). No irreversible degradation in  $J_c$  is measured under axial compression in the experiment. The solid data points represent samples with added copper stabilizer, which is indicated in the legend of both graphs by “+Cu.” The solid lines describe the power-law function:  $J_c(\varepsilon)/J_c(\varepsilon_0) = 1 - a|\varepsilon_0|^{2.2}$ . Values of the strain-sensitivity parameter  $a$  are included in the figure.

full reversibility of the effect is confirmed by unloading the sample and remeasuring  $J_c$  at zero applied strain. Under applied tensile strain,  $J_c$  at first increases slightly to a maximum at about 0.1% strain. With further tensile strain,  $J_c$  reversibly decreases up to 0.52% strain ( $\varepsilon_{\text{irr}}$  in Fig. 2), at which strain  $J_c$  starts to degrade irreversibly due to the breakage of the ceramic superconductor.

A similar dependence of  $J_c$  on applied axial strain in self-field was measured in the MOCVD-IBAD and hybrid MOD-RABiTS conductors. The different samples are compared in Fig. 3. Here, the dependence of the superconducting current density on axial strain is plotted over its reversible range for MOCVD-IBAD [Fig. 3(a)] and (hybrid) MOD-RABiTS conductors [Fig. 3(b)] with and without the addition of stabilizing copper. The critical current density is normalized to its peak value and is plotted as a function of intrinsic strain (defined by  $\varepsilon_0 \equiv \varepsilon - \varepsilon_m$ ). The intrinsic strain normalization allows a direct comparison between the samples of different architectures because, during cooldown, the different thermal contraction rates of the nonsuperconducting materials in the conductor (and the bending beam) place the superconducting layer under different compressive prestrains  $\varepsilon_m$  (0.03% for bare MOCVD-IBAD and bare MOD-RABiTS and between 0.08% and 0.11% for copper surround plated or copper laminated conductors).

The strain dependence of  $J_c$  in self-field for the three different types of conductors can be described well by the power-law expression  $J_c(\varepsilon)/J_c(\varepsilon_0)=1-a|\varepsilon_0|^{2.2\pm 0.02}$  in both the compressive and tensile ranges (shown by the solid lines in Fig. 3). The sensitivity of  $J_c$  to strain is expressed by the strain-sensitivity parameter  $a$  ( $a=6918\pm 210$  for MOCVD-IBAD,  $9538\pm 290$  for MOD-RABiTS, and  $8402\pm 250$  for hybrid MOD-RABiTS).

The strain effect is symmetric for compressive and tensile strains. The close fit to this power-law function and the symmetry provide evidence that the mechanism behind the reversible strain effect in YBCO coated conductors is independent of the production process and is an intrinsic feature of the YBCO grain structure (columnar for MOCVD-IBAD and laminar for MOD-RABiTS). A 20%–30% difference in the strain-sensitivity parameter  $a$  is measured between the MOCVD-IBAD and the (hybrid) MOD-RABiTS samples, and of 10% between the bare and the copper laminated MOD-RABiTS samples. This variation may be caused by differences in the properties of the YBCO layer, such as average grain alignment or grain boundary morphology.

Although we do not rule out any intragranular contributions, a possible mechanism for the reversible strain effect in self-field may be reversible strain fields surrounding dislocations located at the grain boundaries, which arise from the lattice mismatch of adjacent grains.<sup>1,8</sup> These strain fields have a direct effect on the superconducting properties of the material through the superconducting order parameter and a change in charge carrier concentration.<sup>19,20</sup> The results presented here support this picture. For instance, additions of Dy do not significantly affect the strain sensitivity of  $J_c$  in self-magnetic field. Dy additions enhance the flux pinning of the superconductor by changing the intragrain properties of the YBCO layer in MOD-RABiTS, but have no significant effect of the YBCO grain boundaries when no external magnetic field is applied.

We have measured a remarkably large reversible strain effect in highly aligned  $\text{YBa}_2\text{Cu}_3\text{O}_{7-\delta}$  coated conductors through the use of a newly developed measurement technique that allows the superconducting properties to be probed over a wide strain range. The magnitude of the effect will have a significant impact on the design of applications. These results are expected to lead to significant detailed studies into the origin of the reversible strain effect and also indicate that strain may be a useful new parameter for probing the nature of current transport in highly aligned multi-granular HTS materials.

The authors thank SuperPower Inc. and American Superconductor Corporation for providing the samples studied and David McColskey at NIST for providing them with a four-point bender. This work was supported in part by the U.S. Department of Energy, Office of Energy Delivery and Energy Reliability. This work is also a contribution of NIST, a U.S. government agency, not subject to copyright.

<sup>1</sup>D. C. Larbalestier, A. Gurevich, D. M. Feldmann, and A. A. Polyanskii, *Nature (London)* **414**, 368 (2001).

<sup>2</sup>V. Selvamanickam, Y. Chen, X. Xiong, Y. Y. Xie, J. L. Reeves, X. Zhang, Y. Qiao, T. M. Salagaj, Y. Li, K. P. Lenseth, and R. M. Schmidt, *IEEE Trans. Appl. Supercond.* (to be published).

<sup>3</sup>T. Haugan, P. N. Barnes, R. Wheeler, F. Meisenkothen, and M. Sumption, *Nature (London)* **430**, 867 (2004).

<sup>4</sup>N. Long, N. Strickland, B. Chapman, N. Ross, J. Xia, X. Li, W. Zhang, T. Kodenkandath, Y. Huang, and M. Rupich, *Supercond. Sci. Technol.* **18**, S405 (2005).

<sup>5</sup>X. Song, Z. Ch, S. Kim, D. M. Feldmann, D. C. Larbalestier, J. Reeves, Y. Xie, and V. Selvamanickam, *Appl. Phys. Lett.* **88**, 212508 (2006).

<sup>6</sup>J. W. Ekin, D. K. Finnemore, Q. Li, J. Tenbrink, and W. Carter, *Appl. Phys. Lett.* **61**, 858 (1992).

<sup>7</sup>D. C. van der Laan, J. W. Ekin, H. J. N. van Eck, M. Dhallé, B. ten Haken, M. W. Davidson, and J. Schwartz, *Appl. Phys. Lett.* **88**, 022511 (2006).

<sup>8</sup>N. Cheggour, J. W. Ekin, C. C. Clickner, D. T. Verebelyi, C. L. H. Thieme, R. Feenstra, and A. Goyal, *Appl. Phys. Lett.* **83**, 4223 (2003).

<sup>9</sup>N. Cheggour, J. W. Ekin, C. L. H. Thieme, Y.-Y. Xie, V. Selvamanickam, and R. Feenstra, *Supercond. Sci. Technol.* **18**, S319 (2005).

<sup>10</sup>M. Sugano, K. Osamura, W. Prusseit, R. Semerad, K. Itoh, and T. Kiyoshi, *Supercond. Sci. Technol.* **18**, 369 (2005).

<sup>11</sup>V. Selvamanickam, *IEEE Trans. Appl. Supercond.* **11**, 3379 (2001).

<sup>12</sup>V. Selvamanickam, Y. Xie, J. Reeves, and Y. Chen, *MRS Bull.* **29**, 579 (2004).

<sup>13</sup>J. R. Groves, P. N. Arendt, H. Kung, S. R. Foltyn, R. F. DePaula, L. A. Emmert, J. G. Storer, *IEEE Trans. Appl. Supercond.* **11**, 2822 (2001).

<sup>14</sup>D. T. Verebelyi, U. Schoop, C. L. H. Thieme, X. Li, W. Zhang, T. Kodenkandath, A. P. Malozemoff, N. Nguyen, E. Siegal, D. Buczek, J. Lynch, J. Scudiere, M. Rupich, A. Goyal, E. D. Specht, P. Martin, and M. Paranthaman, *Supercond. Sci. Technol.* **16**, L19 (2003).

<sup>15</sup>M. W. Rupich, D. T. Verebelyi, W. Zhang, T. Kodenkandath, and X. P. Li, *MRS Bull.* **29**, 572 (2004).

<sup>16</sup>D. M. Feldmann, T. G. Holesinger, C. Cantoni, R. Feenstra, N. A. Nelson, D. C. Larbalestier, D. T. Verebelyi, X. Li, and M. Rupich, *J. Mater. Res.* **21**, 923 (2006).

<sup>17</sup>A. Goyal, D. P. Norton, J. D. Budai, M. Paranthaman, E. D. Specht, D. M. Kroeger, D. K. Christen, Q. He, B. Saffian, F. A. List, D. F. Lee, P. M. Martin, C. E. Klabunde, E. Hartfield, and V. K. Sikka, *Appl. Phys. Lett.* **69**, 1795 (1996).

<sup>18</sup>D. P. Norton, A. Goyal, J. D. Budai, D. K. Christen, D. M. Kroeger, E. D. Specht, Q. He, B. Saffian, M. Paranthaman, C. E. Klabunde, D. F. Lee, B. C. Sales, and F. A. List, *Science* **274**, 755 (1996).

<sup>19</sup>A. Gurevich and E. A. Pashitskii, *Phys. Rev. B* **57**, 13878 (1998).

<sup>20</sup>R. F. Klie, J. P. Buban, M. Varela, A. Franceschetti, C. Jooss, Y. Zhu, N. D. Browning, S. T. Pantelides, and J. Pennycook, *Nature (London)* **435**, 475 (2005).